

1986

Use of a Simulation Model for Theoretical Optimization Analysis of a Rolling-Piston Type Rotary Compressor

C.M. Franco da Costa

Follow this and additional works at: <https://docs.lib.purdue.edu/icec>

da Costa, C.M. Franco, "Use of a Simulation Model for Theoretical Optimization Analysis of a Rolling-Piston Type Rotary Compressor" (1986). *International Compressor Engineering Conference*. Paper 573.
<https://docs.lib.purdue.edu/icec/573>

This document has been made available through Purdue e-Pubs, a service of the Purdue University Libraries. Please contact epubs@purdue.edu for additional information.

Complete proceedings may be acquired in print and on CD-ROM directly from the Ray W. Herrick Laboratories at <https://engineering.purdue.edu/Herrick/Events/orderlit.html>

USE OF A SIMULATION MODEL FOR THEORETICAL OPTIMIZATION ANALYSIS
OF A ROLLING-PISTON TYPE ROTARY COMPRESSOR

Caio Mário Franco da Costa, M.Sc.

Embraco - Empresa Brasileira de Compressoes S/A
Joinville - SC - 89200 - Brazil

ABSTRACT

A theoretical analysis for the optimization of a refrigeration rolling-piston compressor is presented. A proven simulation program is used as optimization tool. The program equations are examined in detail and its data has been taken from a 650 BTU/hr compressor with representative design. The optimization is studied at characteristic dimensions of the pump (cylinder diameter and height) and at the clearances between the moving parts. The corresponding performance curves: EER, capacity and power input were obtained by varying each of the said parameters in the program data. In order to get a comprehensive explanation for the different performances, each specific energy and mass loss variation is examined in detail. Comments concerning the possibility of using the optimized parameters in practice are made.

INTRODUCTION

This work presents a theoretical optimization analysis of various design parameters of a rolling-piston type rotary compressor. A simulation model is used as optimization tool. The model is based on the calculation of the energy and mass losses that occur during the compression cycle. The losses are calculated instantaneously within small single intervals and integrated for the complete cycle. The calculated mass losses are: suction heating loss, leakage past the contact point, leakage past the blade edges and absorption of gas in oil. The calculated energy losses are: those caused by the compression of the gas leakage and of the gas absorbed in oil; those caused by friction between the moving parts inside the cylinder and at the bearing; those due to the geometrical design: over-compression loss and top-clearance loss; and others: oil heating of the gas, motor loss and windage loss. Based on the equation of the moments, the instantaneous absolute angular velocity of the roller is calculated. To prove the suitability of

the program the numerical results of the performance curves (EER, capacity and power input) for a 650 BTU/hr compressor and the actual performance curves of the very same compressor obtained in calorimeter tests were compared for various load conditions.

As the program proved to give good results, it was used for a theoretical optimization analysis. The following parameters are examined: the characteristic dimensions of the pump (cylinder diameter, cylinder height, roller diameter); the clearances between the moving parts, and the angle of the discharge port. The analysis procedure was made changing the reference parameter within a given range, keeping every other parameter constant. The results are presented by the variation of the EER, capacity and power input, at the check point condition. In order to get a comprehensive explanation for the different performances, each specific energy and mass loss variation is examined in detail.

SIMULATION MODEL

MASS LOSSES

Gas Leakage Losses

The main leakage losses are past the contact point and past the blade edges. Both leakages can be modelled as isentropic flow through a convergent - divergent nozzle:

$$\dot{m}(\theta) = A_c p_c(\theta) \left[\frac{k-1}{2} M^2 + 1 \right]^{(1/1-k)} M \sqrt{k/RT(\theta) \left(M^2 \frac{k-1}{2} + 1 \right)} \quad (1)$$

We concluded that there is an oil seal at the contact point between roller and cylinder, because of this the flow past the minimal clearance will occur only after the pressure difference between the two chambers is high enough to break this oil seal. This leakage is given by:

$$\dot{m}_c(\theta) = 0; p_c(\theta) < P_{\min} \quad \text{for seal breaking} \quad (2)$$

$$\dot{m}_c(\theta) = \psi_c (\delta_c(\theta) - \xi) h_c \dot{m}(\theta); p_c(\theta) \geq P_{\min}$$

Due to the characteristic movement of the blade, no oil seal will be formed on it. Hence the leakage past the blade edges may be assumed to occur during the entire compression cycle. This leakage is given by:

$$\dot{m}_b = 2 \psi_b \delta_b h_b \dot{m}(\theta) \quad (3)$$

ENERGY LOSSES

Leakages Compression Loss

Gas leakages past the cylinder clearances from the compression to the suction chamber occurs during the whole cycle; as described above. Obviously this gas is partially compressed before it leaks from the compression chamber. So it has also to be accounted as an

energy loss. The following equation gives the instantaneous loss for leaked gas compression:

$$\dot{E}_{lc1} = (H_c(\theta) - H_s) (\dot{m}_c(\theta) + \dot{m}_b(\theta)) \quad (4)$$

Oil Heating Loss

The oil that penetrates into the cylinder is at a relatively high temperature, hence when in contact with the oil the gas inside the cylinder is heated up. This heating obviously increases the required compression work. This energy loss is given by equation:

$$\dot{E}_{ohl} = (\dot{m}_{or}(\theta) + \dot{m}_{ob}(\theta)) C_{po} (T_o - T(\theta)) \quad (5)$$

The oil penetrates into the cylinder in two ways

- through the roller head clearances

$$\dot{m}_{or} = \frac{\rho_o (\delta_r/2)^3 (p_d - p(\theta))}{12 \mu_o \ln(R_r/R_e)} \quad (6)$$

- through the blade sides

$$\dot{m}_{ob} = \frac{\rho_o (\delta_b)^3 h_b (p_d - p(\theta))}{12 \mu_o l_b} \quad (7)$$

Over Compression Loss

To calculate the over-compression loss we have chosen a procedure (Eq. 8) that, in spite of being a simplified one, gave reasonable results within the desired precision. It is the same as to approach the actual work loss during over-compression by the triangle (Vc Vb, Pd Pj). See fig. 11.

$$\dot{E}_{vcl} = \frac{N}{120} (V_b - V_c) (P_j - P_d) \quad (8)$$

The peak pressure P_j can be assumed proportional to the relation between the valve area and the valve port area.

Angular Velocity of the Roller

In order to improve the accuracy of the simulation the absolute angular velocity of the roller must be calculated instantaneously during the piston revolution. Solving the equation of the moments:

$$I \dot{\omega}_p + M_c + M_b + M_r = 0 \quad (9)$$

through a simple numerical procedure one can get ω_p (shown in fig. 1 for "check-point" condition and 3497 rpm). Most of the friction losses are related with ω_p .

Friction Losses

The friction losses are calculated using the following modeling:

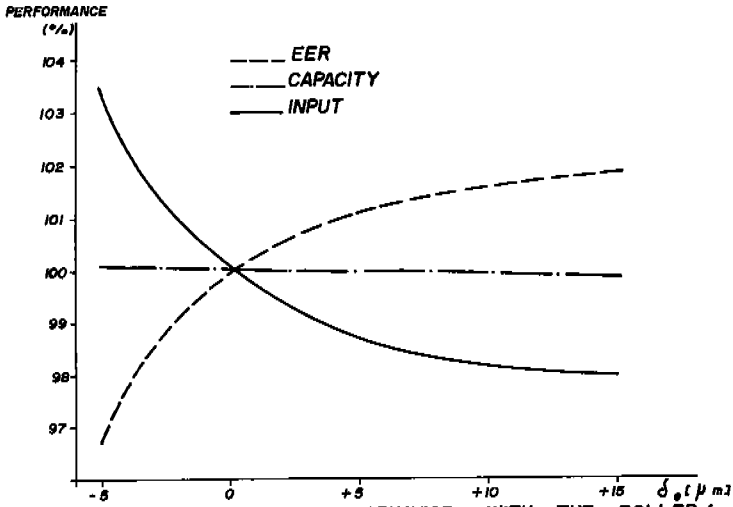


FIG.6.a - PERFORMANCE CURVES BEHAVIOR WITH THE ROLLER/ECCENTRIC CLEARANCE VARIATION.

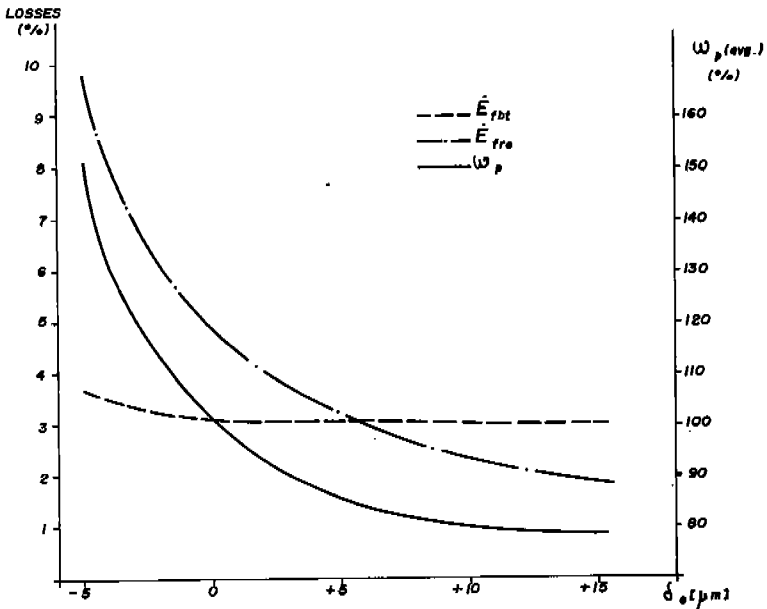


FIG.6.b - INDIVIDUAL LOSSES AND ROLLER AVERAGE ABSOLUTE ANGULAR VELOCITY BEHAVIOR WITH ROLLER/ECCENTRIC CLEARANCE VARIATION.

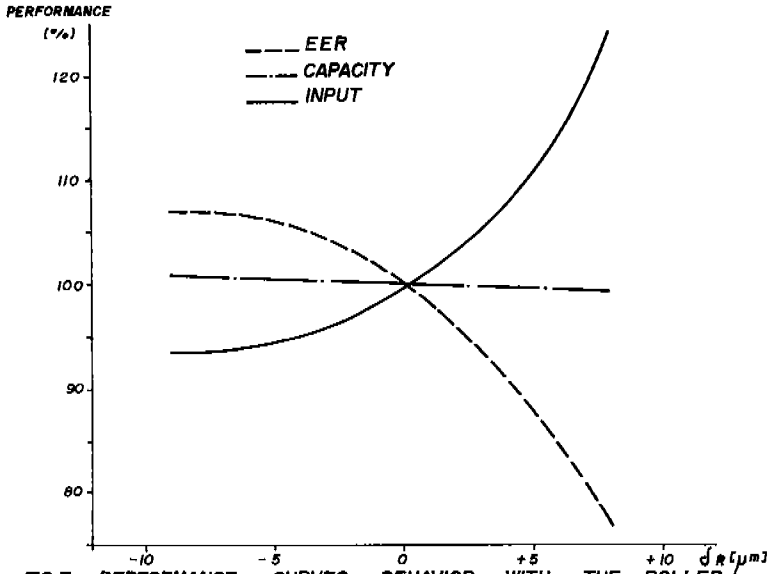


FIG. 7.a - PERFORMANCE CURVES BEHAVIOR WITH THE ROLLER HEAD CLEARANCE VARIATION.

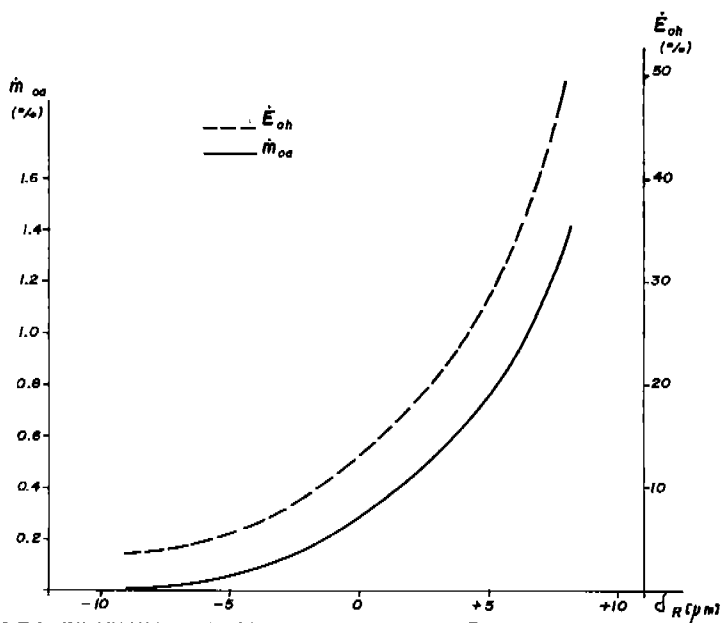


FIG. 7.b - INDIVIDUAL LOSSES BEHAVIOR WITH THE ROLLER HEAD CLEARANCE VARIATION.

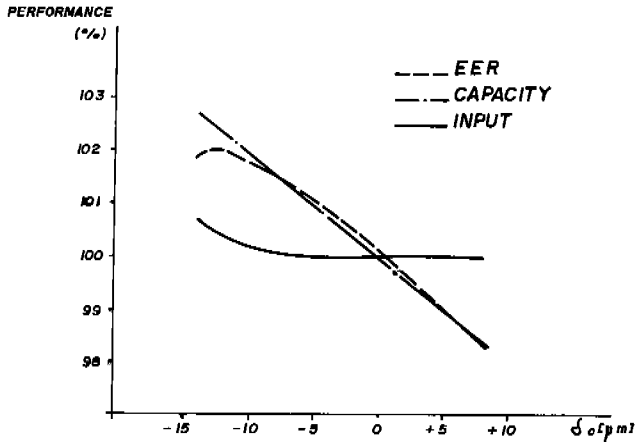


FIG.8.a - PERFORMANCE CURVES BEHAVIOR WITH THE MINIMAL CLEARANCE VARIATION.

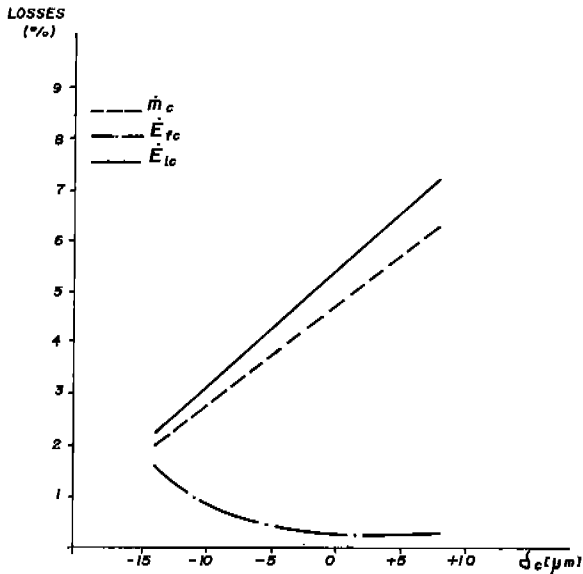


FIG.8.b - INDIVIDUAL LOSSES BEHAVIOR WITH THE MINIMAL CLEARANCE VARIATION.

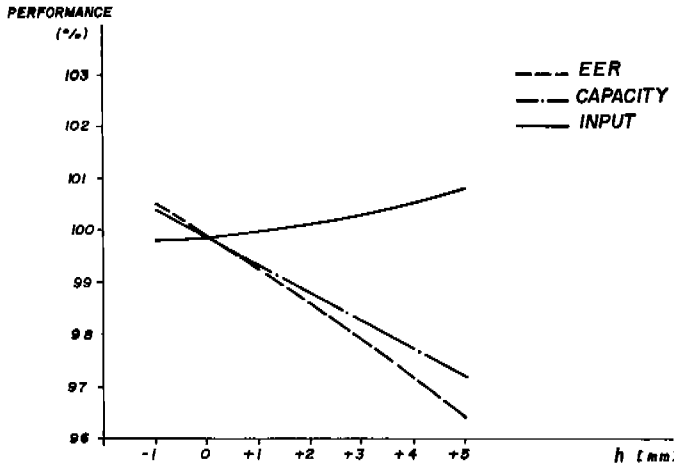


FIG.9.a - PERFORMANCE CURVES BEHAVIOR WITH THE CYLINDER HEIGHT VARIATION.

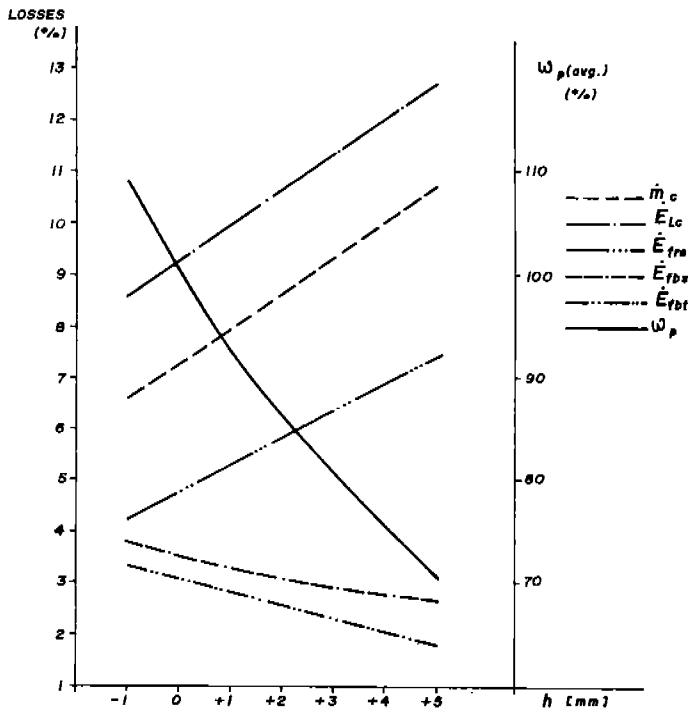


FIG.9.b - INDIVIDUAL LOSSES AND ROLLER AVERAGE ABSOLUTE ANGULAR VELOCITY BEHAVIOR WITH THE CYLINDER HEIGHT VARIATION.

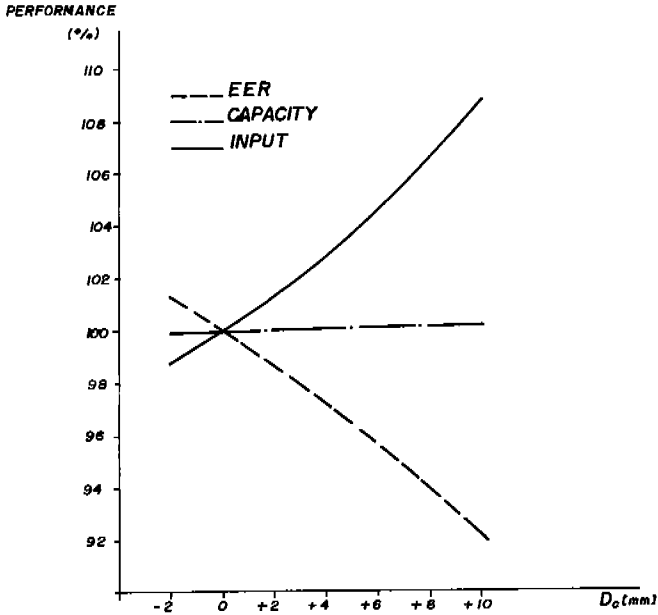


FIG. 10.a - PERFORMANCE CURVES BEHAVIOR WITH THE CYLINDER DIAMETER VARIATION.

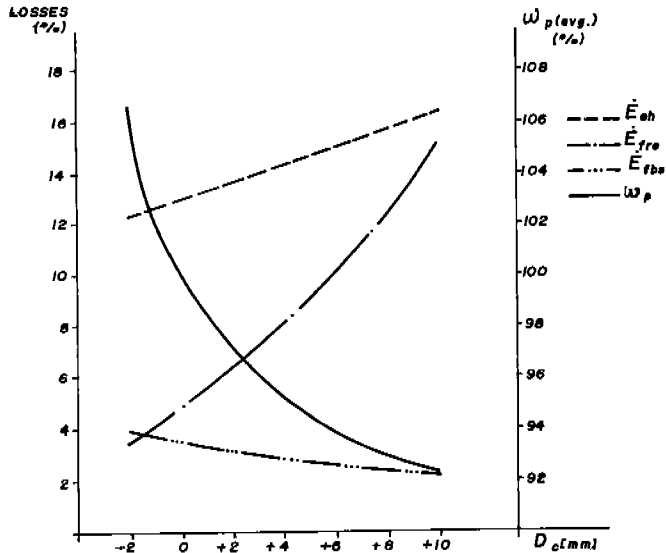


FIG. 10.b - INDIVIDUAL LOSSES AND ROLLER AVERAGE ABSOLUTE ANGULAR VELOCITY BEHAVIOR WITH CYLINDER DIAMETER VARIATION.

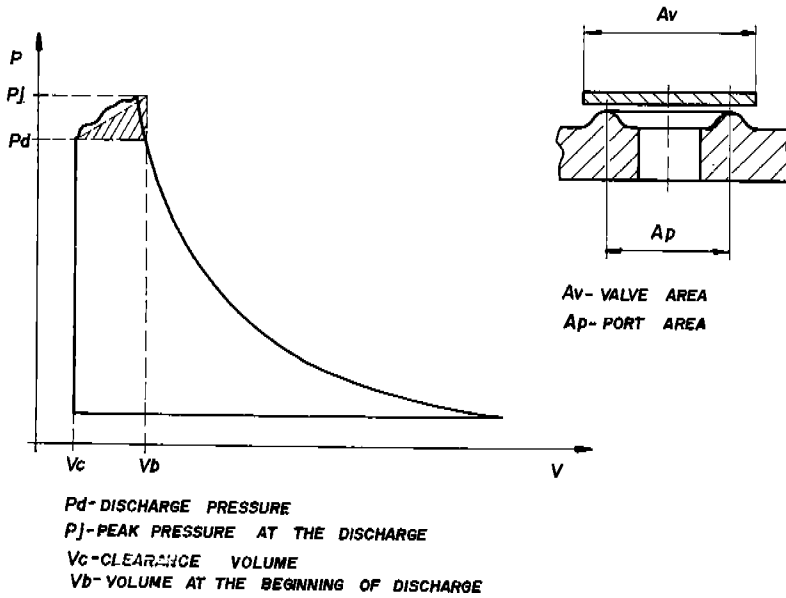


FIG.11 - OVER - COMPRESSION LOSS

VOLUMETRIC EFFICIENCY	% OF MASS FLOW
- SUCTION HEATING LOSS	0,37
- LEAKAGE AT CONTACT POINT	5,20
- LEAKAGE AT BLADE EDGES	2,05
- GAS IN OIL ABSORPTION LOSS	0,38
ENERGETIC EFFICIENCY	% OF POWER INPUT
- BEARINGS FRICTION LOSS	2,42
- BLADE TIP FRICTION LOSS	1,46
- ROLLER/ECCENTRIC FRICTION LOSS	2,70
- BLADE SLOT FRICTION LOSS	2,19
- OVER-COMPRESSION LOSS	2,57
- TOP-CLEARANCE LOSS	2,23
- WINDAGE LOSS	0,66
- OIL HEATING LOSS	6,01
- LEAKED GAS COMPRESSION	3,41
- MOTOR LOSS	26,80
- OTHER LOSSES	0,48

TABLE.2- CALCULATED ENERGY AND MASS LOSSES AT CHECK-POINT CONDITION.

Friction Loss	Model
. Bearing friction loss	Hidrodynamic lubrication
. Blade tip friction loss	Contact lubrication
. Blade slot friction loss	Contact lubrication
. Roller/eccentric friction loss	Viscous drag
. Roller head friction loss	Lubrication in parallel discs

Table 1 - Friction losses modeling

Results

Introducing the data for a 650 BTU/hr rolling-piston compressor into the program derived from the above losses analysis, we had the following results shown in table 2. A comparison between the program output and actual calorimeter performance curves is shown by figures 2 to 4 for conditions over the 559C condensing temperature. It can be noticed that the program results fit the curves over their entire scope. Therefore, the said program may be used as reasonable design optimization tool.

DESIGN OPTIMIZATION

Variation of the Discharge Port Angle

Reducing the discharge port angle (θ_d) by bringing it closer to the blade slot, taking it as data of the simulation program and keeping constant every other parameter, one shall have the curve shown in fig. 5.a*. It shows a very distinct value for the optimization of the EER, with its corresponding capacity and power input. The capacity drops with the discharge angle and, consequently, also the power input required to compress such mass flow. Analyzing the following individual losses in fig. (5.b) one can have a clear idea for such a behavior: (\dot{m}_c) gas leakage at the contact point increases with θ_d , because the greater the distance between the discharge port and the angle of discharge beginning, greater is the angle swept with over-pressure, and consequently, greater is the interval for this loss to occur; (E_{lc}) energy loss to compress the \dot{m}_c mass loss is obviously proportional to \dot{m}_c ; (E_{cv}) top clearance loss, as the discharge angle decreases the space for the clearance volume increases; and indeed, also the energy required to compress such volume.

Variation of the Roller/Eccentric Clearance

While the radial clearance between roller and eccentric (δ_e)

* in the figures that follow it is established that: for the performance curves (EER, capacity and power input) the original performance was taken as 100%; for the energy losses the original adiabatic work was taken as 100%; for the mass losses the original mass flow was taken as 100%; for the average ω_p the original average ω_p was taken as 100%.

is narrow, the EER of the compressor increases steeply. As it expands the EER curve becomes flatter see fig. (6.a). The capacity is almost not affected by this clearance while the power input drops steeply with it. The clearance used in the examined compressor gives poorer efficiency than would be obtained using larger clearances. The reason for this choice depends on life time requirements for the pump. However, in practice one can find compressors with much greater clearance, about 5 μm or more than the one here examined. The individual losses that cause such behavior of the EER are shown in (fig. 6.b). Both are functions of the roller absolute angular velocity (ω_p). Since the velocity ω_p drops as the clearance expands, the said individual losses have the following changes: (E_{fre}) roller/eccentric friction loss drops exponentially as R_e enlarges; (E_{fbt}) blade tip friction loss drops until R_e approximates to $-2\mu\text{m}$, down to this point it continues to drop, although very slightly - dependent of the sliding velocity of the roller u_s which tends to slow down with ω_p .

Variation of the Roller/Cylinder Axial Clearance

This clearance plays perhaps the most critical role in the compressor optimization. Fig. (7.a) shows that the EER of the compressor steeply decreases as the roller/cylinder clearance (δ_r) increases. It is caused by the rapid increase of the power input, while the capacity drops slightly. It happens because δ_r controls most of the oil flow into the cylinder. When the oil penetrates into the cylinder it rises the temperature of the gas, so compression work increases. It is called oil heating loss (E_{oh}). On the other hand, the oil absorbs refrigerant thus decreasing the capacity of the compressor. This loss (\dot{m}_{oa}) is shown in fig. (7.b). However, we know that EER curve shown in fig. (7.a), actually - in practice - will decrease sharply when δ_r becomes smaller than a certain value. It happens when δ_r becomes too narrow to allow enough lubricant oil to penetrate into the cylinder. This lack of oil will facilitate the occurrence of both: metallic contact between the moving parts, and the breaching of the oil seals that avoid free gas leakage between the moving parts. This explain why smaller clearances are not used in actual compressors. These phenomena will mean abnormal working conditions and are not set up in the simulation.

Variation of the Minimal Clearance

As shown in fig. (8.a) the EER decreases as the minimal clearance at the contact point between roller and cylinder walls increases. While the capacity drops constantly, the power input is a bit higher as the clearance gets too narrow, becoming almost constant as the clearances expands. This explains the sharp decrease of the EER curve at the smaller clearances. Such behavior can be understood analyzing the following individual losses, fig. (8.b): (\dot{m}_c) gas leakage at the contact point increases as the leakage path (the clearance δ_c) becomes larger, it explains the decreasing capacity; (E_{lc}) energy loss for compression of \dot{m}_c is obviously proportional to the \dot{m}_c mass loss, this explains why the power does

not fall as the capacity decreases; (E_{fc}) friction loss at the contact point increases as the clearance becomes narrow, elevating the power input. As one may observe the performance could be improved if a smaller clearance could be used. However, in practice a too narrow clearance may cause the hitting of piston at the cylinder walls, and obviously, this must be avoided in the first instance.

Cylinder Height Variation

Varying the cylinder height, keeping the cylinder diameter constant, and calculating the roller diameter as derived dimension, we get Fig. (9.a) for the performance curves. As height increases, the power input grows and the capacity falls, causing the EER to drop fast. In fig.(9.b) one can see that the decrease of the EER is brought about specifically by the following changing losses: (\dot{m}_c) gas leakage past the contact point increases with the height as the area the path for this leakage is enlarged; (E_{lc}) energy loss for compression of \dot{m}_c leakage is proportional to the \dot{m}_c leakage; (E_{fre}) roller/eccentric friction loss increases as the contact area increases with h , and also due to the increases of ω_r ; (E_{fbs}) blade slot friction loss decreases with the eccentricity of the roller; (E_{fbs}) blade tip friction loss decreases with the sliding velocity u_s .

Variation of the Cylinder Diameter

Varying the cylinder diameter, keeping the height constant, and calculating the roller diameter as a derived dimension, we get the diagram shown in fig. (10.a) for the performance curves. As the diameter expands, the power input grows steeply and the capacity keeps almost constant. Consequently the EER will fall rapidly. Fig. (10.b) shows the specific varying losses that result in the said behavior: (E_{oh}) oil heating loss increases as the ratio R_r/R_e decreases; (E_{fre}) roller/eccentric friction loss increases as the contact area increases with R and also due to the increase of ω_r ; (E_{fbs}) blade/slot friction loss decreases with the eccentricity of the roller.

CONCLUSIONS

The optimization analysis of various design parameters were presented. The best range for the optimization of each dimension could be spotted. For every case the losses basically responsible for the performance behavior were studied in detail. This gives a clear idea of how the changes in the performance occur. The simulation program used, in spite of a simplified over compression loss equationing, gave satisfactory results. The use of the instantaneous angular velocity of the roller improved the program accuracy, making it possible to calculate all the related losses during every step of the cycle.

SYMBOLS

A_c - minimal clearance area; C_p - specific heat; D - diameter; H - enthalpy; h - cylinder height; h_b - blade height; I - moment of inertia; k - specific heats ratio; L - work; l - length; M - flow mach number; M_e - roller/eccentric viscous moment; M_b - blade tip moment; M_r - roller head viscous moment; \dot{m} - mass flow; N -rpm; n - politropic exponent; P - pressure; $p(\theta)$ - compression instantaneous pressure; R - radius; T - temperature; U - overall heat transfer coefficient; u - roller/blade sliding velocity; V - volume; V_c - top-clearance volume; δ_c - minimal clearance; δ_b - blade head clearance; δ_r - roller head clearance; ξ - oil film thickness Δ_c - difference of refrigerant in oil concentration at the pump and cylinder conditions; θ - roller revolution instantaneous angle μ_o - oil viscosity; ρ_o - oil density; ψ - nozzle coefficient; ω_p - roller angular velocity; ω_r - roller/eccentric relative angular velocity; ω_s - shaft angular velocity. Subscripts: c - compression, clearance, cylinder; d - discharge; e - eccentric; o - oil; r - roller; s - suction; sl - suction line, b - blade.

REFERENCES

- 1 - PANDEYA, P. and SOEDEL, W. - "Rolling Piston type Rotary Compressors with special Attention to friction and Leakage", PCTC, Purdue Univ. (1978).
- 2 - GYBERG, F. - "A Simulation Model for Fixed Vane Rotary Compressor Using Real Gas Properties", PCTC, Purdue Univ. (1984).
- 3 - SAKURAI, E. and HAMILTON, J. F. - "The Prediction of Frictional Losses in Variable - Speed Rotary Compressors", PCTC, Purdue Univ. (1984).
- 4 - MATSUZAKA, T. - "Rolling Piston Type Rotary Compressor Performance Analysis", PCTC, Purdue Univ. (1982).
- 5 - REED, W. A. and HAMILTON, J.F. - "Internal Leakage Effects in Sliding Vane Rotary Compressors", PCTC, Purdue Univ. (1980).
- 6 - YANAGISAWA, T. and SHIMIZU, T. - "Friction Losses in Rolling Piston Type Rotary Compressor III", Int. J. Refrig. 4, 3, (1985).
- 7 - YANAGISAWA, T. and SHIMIZU, T. - "Leakage Losses with a Rolling Piston Type Rotary Compressors II", Int. J. Refrig. 8, 3 (1985).
- 8 - ASAMI, K. et al. - "Improvements of Noise and Efficiency of Rolling Piston Type Refrigeration Compressor for Household Refrigerator and Freezer", PCTC, Purdue Univ. (1982).
- 9 - WAKABAYASHI, H. - "Analysis of Performance in a Rotary Compressor", PCTC, Purdue Univ. (1982).

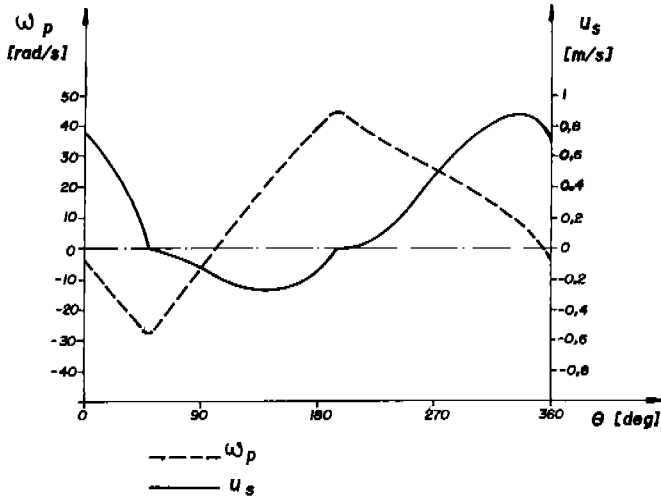


FIG.1 - ABSOLUTE ANGULAR VELOCITY OF THE ROLLER AND SLIDING VELOCITY AT THE BLADE TIP.

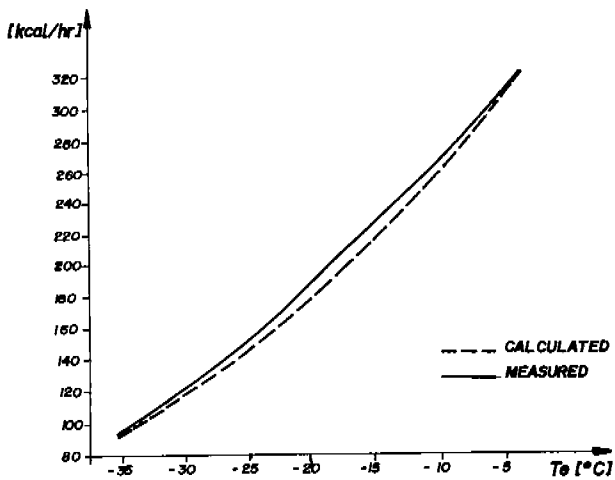


FIG.2 - CAPACITY OVER $T_c = 55^\circ\text{C}$

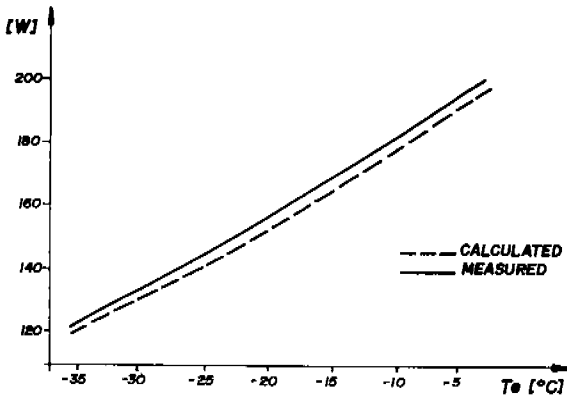


FIG.3- POWER INPUT OVER $T_c=55^\circ\text{C}$

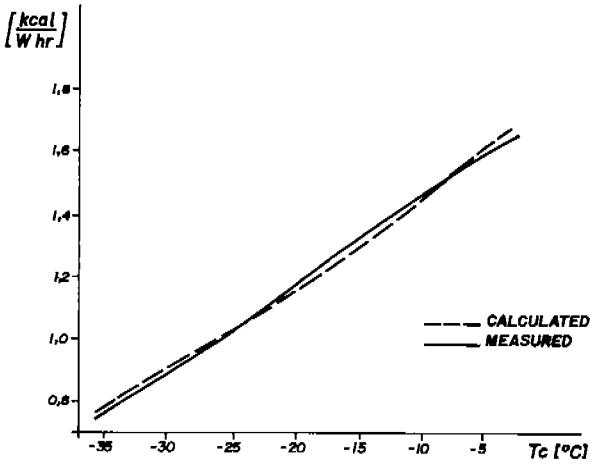


FIG. 4- EER OVER $T_c=55^\circ\text{C}$

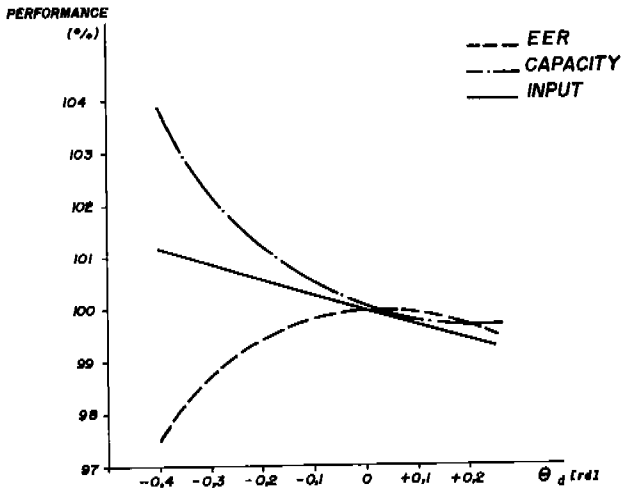


FIG.5.a - PERFORMANCE CURVES BEHAVIOR WITH THE DISCHARGE PORT ANGLE VARIATION.

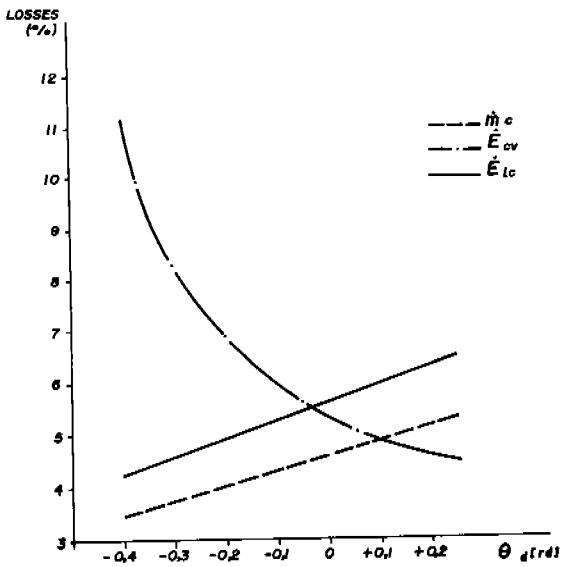


FIG.5.b - INDIVIDUAL LOSSES BEHAVIOR WITH THE DISCHARGE PORT ANGLE VARIATION.